Stability Testing of a Carbon Fiber Composite Optical Bench for Use in the Space Based LIDAR Mission: CALIPSO

Brian Catanzaro[a], Joe Hylton[b], Brian Stumm[b]

[a] CFE Services, 5147 Pacifica Dr., San Diego, CA 92109[1]
[b] Composite Optics, Incorporated

ABSTRACT

The CALIPSO LIDAR is a two-channel visible/infrared, polarization sensitive space based instrument. The mission specifies a lightweight, thermally stable platform for the lasers, 1-m telescope, and LIDAR instrumentation. Stability requirements include ±26 µrad boresight stability between the telescope and the laser as well as ±10 µm optical bench thickness stability and ±70 µm stability of components on the optical bench. The environment for these performance criteria is a 0 C to 50 C space environment. In order to demonstrate performance, a laser tracker, a laser comparator, and an electronic autocollimator were used in conjunction with an environmental chamber to measure the stability of the structure over the operating temperature range.

Keywords: LIDAR, composite, carbon fiber, low thermal expansion, space based optics

1. CALIPSO LIDAR

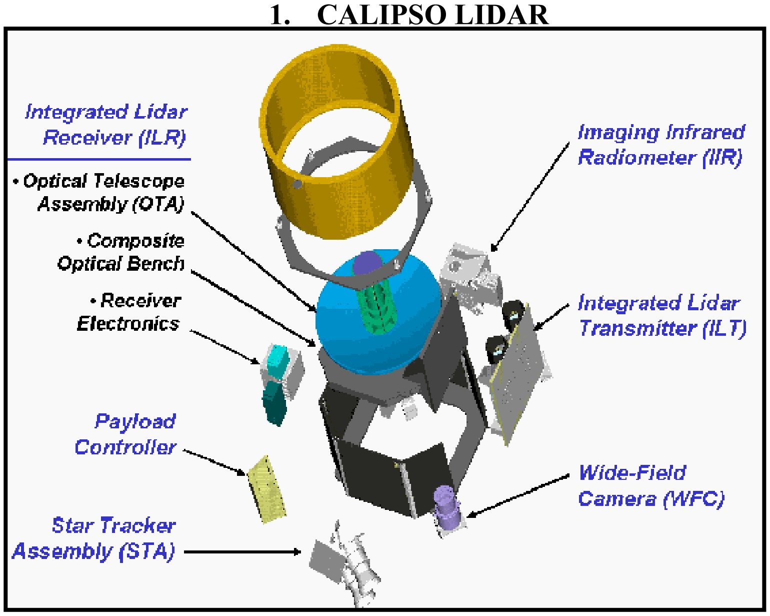

Figure 1: CALIPSO LIDAR

The instrumentation for the Cloud-Aerosol Lidar and Infrared Pathfinder Satellite Observatory (CALIPSO) mission is two wavelength, dual polarization LIDAR. The system includes an integrated laser illumination system, a 1-m beryllium light collection telescope, imaging sub-systems, and the LIDAR detection optical system (see Figure 1). The LIDAR was co-developed by Langley Research Center (NASA – LaRC) and Ball Aerospace (BATC). The platform that supports the telescope, lasers, LIDAR detection system, and imaging sub-systems is a carbon fiber reinforced composite (CFRC) stable structure (see Figure 2) designed and manufactured by Composite Optics, Incorporated (COI).

---

[1] Correspondence - Email: bcatanza@alumni.caltech.edu; Telephone: 858-204-6299

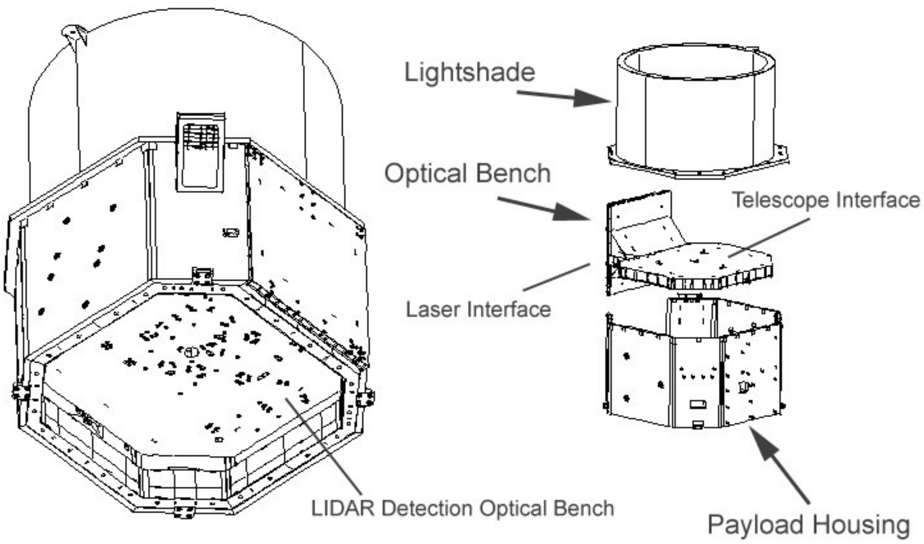

Figure 2: CFRC Stable Structure for CALIPSO LIDAR

The CFRC stable structure maintains the alignment of several key components in the LIDAR. An allocation of the entire budget for performance was made to the CFRC structure. The allocation for stability of the components on the LIDAR detection optical bench controlled by linear distortion of the CFRC structure is: ±70 μm. The allocation for the stability of the distance between the telescope focal point and the LIDAR detection optical system is controlled by an optical bench thickness specification: ±10 μm. The allocation for the stability of the angle between the laser interface and the telescope interface controlled by the CFRC structure is: ±26 μrad. These specifications are to be maintained over the operating conditions of 0 C to 50 C.

The CFRC structure was manufactured from high stiffness, low thermal expansion (-0.15 ppm/C $< \alpha < 0$ ppm/C), low outgassing laminates. The design incorporated metallic fittings integrally bonded to the structure. The optical bench was connected to the payload housing using flexures.

2. TEST OBJECTIVES

In an effort to demonstrate the performance of the structure under operating conditions, a test was defined. The purpose of the test was to characterize the performance of the CFRC structure prior to the integration of any LIDAR components. The test objectives were to monitor the performance of the optical bench stability, optical bench thickness, and telescope/laser boresight stability over the 0 C to 50 C temperature range. The test was not required to be performed in vacuum. However, since CFRC structures absorb/desorb moisture, the structure had to be dry prior thermal stability testing. The measurement points for the various tests were defined to mimic the actual components that would be mounted to the various interfaces. Therefore, it was critical to provide fixturing that simulated not only kinematic mounted, but also the same constrained degrees of freedom as the flight hardware.

3. TEST INSTRUMENTATION

Each of the three characteristics was measured using different techniques. The stability of the optical bench was measured using a laser tracker. The stability of the thickness of the optical bench was measured using a laser optical comparator. The boresight stability was measured using an electronic autocollimator.

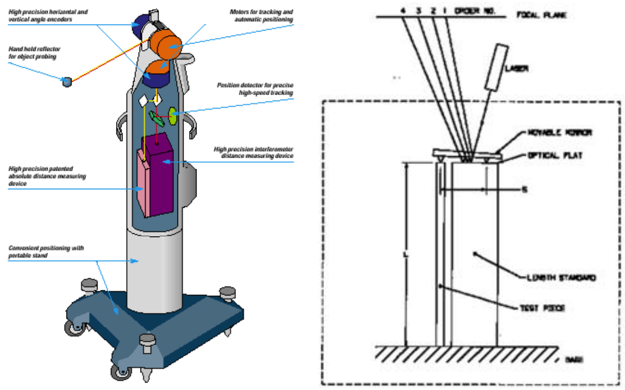

Figure 3: Leica Laser Tracker LTD 500 (left) – COI Laser Optical Comparator (right)

Laser tracker technology is based on angular encoders and optical distance measurement. The particular laser tracker selected for this test was the Leica LTD 500 (see Figure 3). This device uses a corner cube as a reference. The laser tracker projects a tracking signal which is retroreflected by the corner cube. Each measurement is an average of 100 measurements. Azimuth and elevation encoders use the centroid of the return signal and determine the direction of the corner cube. The laser tracker has two methods for determining distance: a laser distance interferometer (LDI) and a time of flight (TOF) measurement. These methods compensate for index of refraction changes in the environment by monitoring temperature, humidity, and pressure. The LDI technique requires constant monitoring of the return signal. Given the configuration of the test, this was not practical. Instead, the test relied on the TOF measurement. The instrument was compared with a coordinate measurement machine (certified ±5 µm), an HP LDI (certified < ±1 µm), and a precision vernier (±1 µm). In absolute measurement capability, the laser tracker accuracy was better than ±17 µm. In a stability test, highly accurate absolute measurement is not necessarily required. More often, the structure experiences slight changes in dimension. Therefore, the relative motion of interfaces is more important than their absolute distance. In tests designed to measure relative motion, the laser tracker matched the coordinate measuring machine, HP LDI, and vernier to within ±5 µm.

The optical laser comparator technique was pioneered by COI to measure small displacements with respect to a reference standard. The technique uses small mirror that rests on both the standard and the object under test (see Figure 3). When the object under test grows (shrinks) due to changes in the environment, the mirror rotates. The angle of the mirror can be measured by reflecting a laser off of the mirror. By using a small mirror and placing the two objects in close proximity, the measurement can become very sensitive. This technique has been compared with NIST measurements of thermal expansion. The accuracy of the technique is better than ±0.5 µm.

Autocollimator technology is commonly used to measure angles in optical components and systems. The instrument selected for this test was the Elcomat HR. This instrument provides two axis measurements. Data collection is performed through a computer interface and rates are limited to 20 Hz. Typical application included the collection of 200 data points for each measurement. The nominal accuracy of the instrument is better than ±0.2 µrad.

Figure 4: Thermal Chamber Test Run (left), Support Tower (middle), Structure During Test Integration (right)

A chamber was constructed to dry, heat, and cool the structure. This chamber was designed to operate at ambient pressure with an environment of dry nitrogen. A closed loop system was used to monitor and control the temperature. Over 30 thermocouples were distributed throughout the structure, chamber, heating, and cooling systems. Optical windows (BK7, Transmitted WFE < $\lambda/4$ RMS) were placed on the top surface of the chamber to allow the instruments to be located outside the chamber.

4. TEST CONFIGURATION

All of the tests were performed in the same chamber. However, each measurement used a slightly unique configuration.

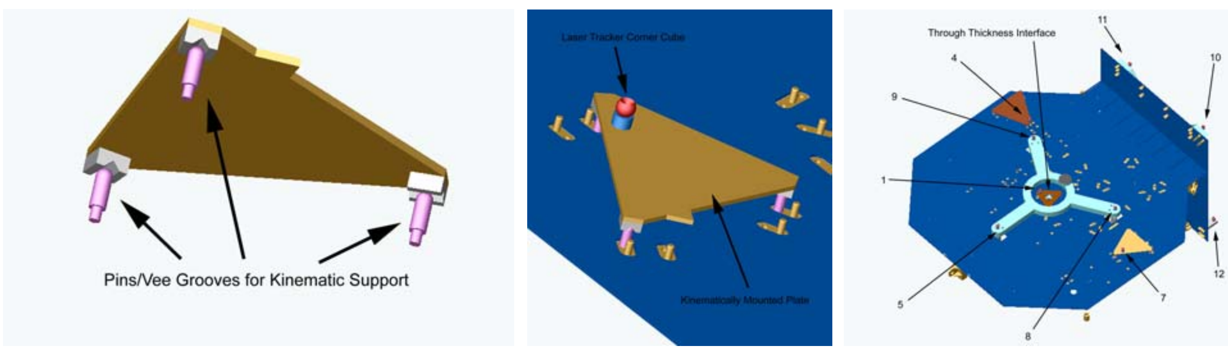

Figure 5: Reference Fixtures for Laser Tracker Corner Cubes

The test for the stability of the optical bench was configured using the laser tracker viewing a series of retroreflectors through a window in the chamber. The retroreflectors were mounted to the structure using reference fixtures. All of the reference fixtures on the optical bench were kinematically mounted to the structure. The reference fixtures consisted of a small invar plate with a corner cube mounted on one side and vee-grooves on the other. The vee-grooves interfaced with pins that were threaded into the fittings on the structure (see Figure 5). The orientation of the vee-grooves matched the orientation of compliance of the flexure mounts of the components which would later be integrated to the LIDAR. These reference fixtures were distributed across the surface of the optical bench. Due to the limited number of corner cubes, not all of the locations could be measured in a single thermal cycle. Therefore, this portion of the test was conducted in two phases.

Although the laser tracker allowed the input of temperature, humidity, and pressure data to compensate for environmental conditions, this feature could only be used to a limited extent for this test. The laser tracker was located outside of the chamber. As such, it could compensate for the environment in the lab, but not the chamber. The hot (cold) air inside the chamber can cause several errors: transient gradients can cause random errors, bulk temperature change causes errors in the optical path, refraction at the window/hot (cold) interface causes azimuth/elevation errors.

Given the experience with similar chambers, the gradient was anticipated to be less than ±3 C. The ranging error can be derived from the value of dn/dT for air (0.96 ppm/C). The average range was 2 m. This resulted in an error of approximately: ± 5.8 μm. The errors from bulk temperature changes in the environment were large enough that they exceeded the accuracy requirement; they had to be calibrated out of the test data. The solution was to instrument a large stable reference inside the chamber and scale all data to that reference. As will be described later, a large ULE^{TM} reference structure was kinematically mounted to the structure. This was instrumented with corner cubes and all data was best-fit to the values from this structure.

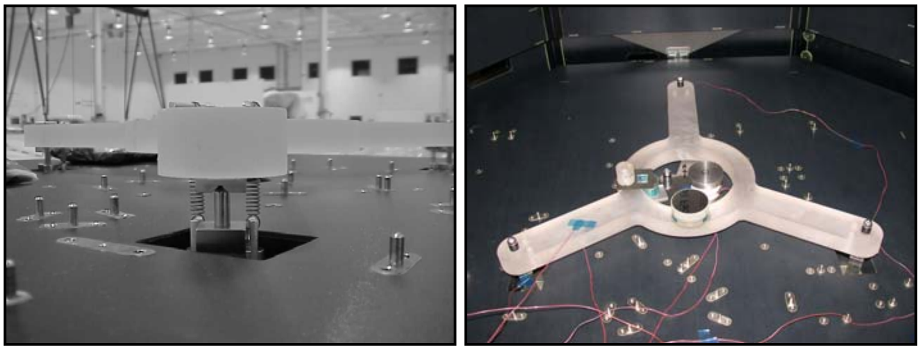

Figure 6: Reference Fixture to Telescope Interface – Kinematic Interface (left), Test Configuration (right)

The optical bench thickness measurement required referencing to the telescope interfaces and interfaces on the optical instrument side of the optical bench. The optical bench is essentially a hollow sandwich structure. The interface fittings for the telescope are bonded to support ribs. The fittings for the telescope can be accessed from the instrument side of the optical bench, so the reference fixture for the telescope interfaces can be placed on the same side as the instrument reference fixture. However, the footprint of the interfaces was on a circle 0.5 m in diameter. Referencing only one of the three interfaces would not have resulted in an accurate representation of the performance of the structure. Therefore, a reference fixture had to be developed to mate to all three of the telescope interfaces. Due to the precision of the measurement and the range of temperature, the reference fixture had to be designed with the same kinematic interface designed for the telescope. ULE^{TM} was selected as the material for the interface. Using a proprietary technique developed at COI, remnant ULE^{TM} was flowed into a 0.6 m x 0.6 m x 0.025 m substrate. This was subsequently ground flat and waterjet machined to shape. Invar vee-grooves were bonded to the fixture and oriented at 120^{o} angles. These grooves were mated to pins on posts that were bolted to the telescope interfaces on the structure (see Figure 6). This combination of pins and vee-grooves provided a kinematic support over the entire temperature range. The reference fixture for the interfaces to the optical instrument side of the bench was designed in a similar fashion. However, since the distance between interface fittings is much smaller (less than 75 mm) so invar was chosen for the reference fixture. The final configuration is shown in Figure 7.

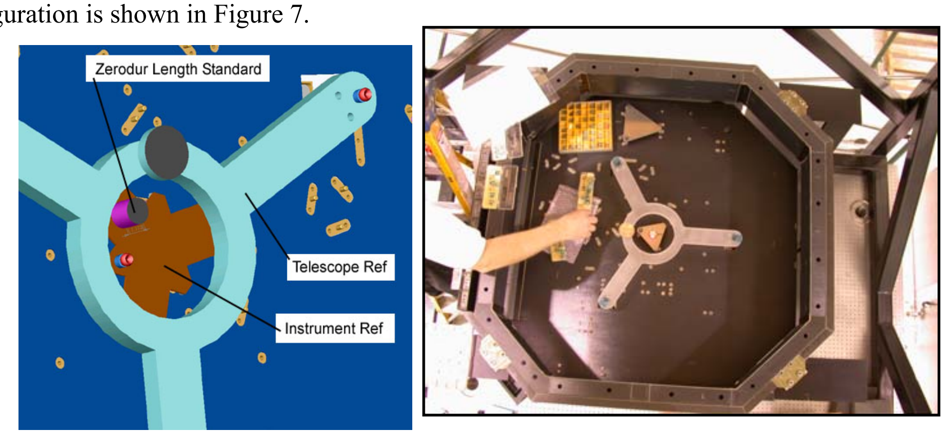

Figure 7: Optical Bench Thickness Test Configuration

The measurement of the boresight stability was a complex configuration that included large ULE^{TM} reference fixtures, a periscope, a reference flat, and the electronic autocollimator.

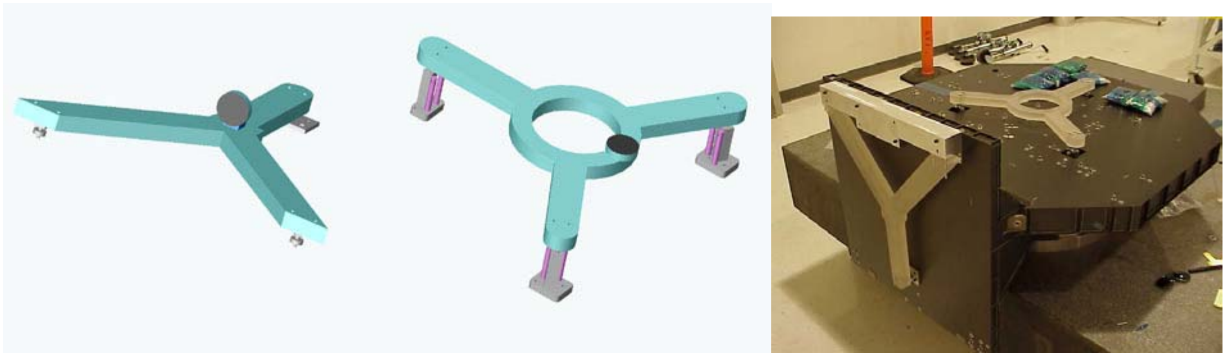

Figure 8: ULE^{TM} Reference Structures for Boresight Stability Measurement (Laser – left, Telescope – middle, Integrated with Structure – right)

The reference fixtures were designed to provide references to the interfaces for the laser and telescope (see Figure 8). The telescope reference has been previously described. In addition to the optical bench thickness tilt mirror, a 50 mm mirror was kinematically mounted to the reference fixture to serve as a target for the autocollimator. A similar reference fixture was designed for the laser interfaces. The laser did not have a simple 120^o kinematic interface. As such, instead of three vee-grooves, a plate, a cone, and a vee-groove were used to constrain the movement of the reference fixture. In addition, since the laser reference fixture was mounted perpendicular to gravity, springs were used as restoring forces to hold the fixture against the structure.

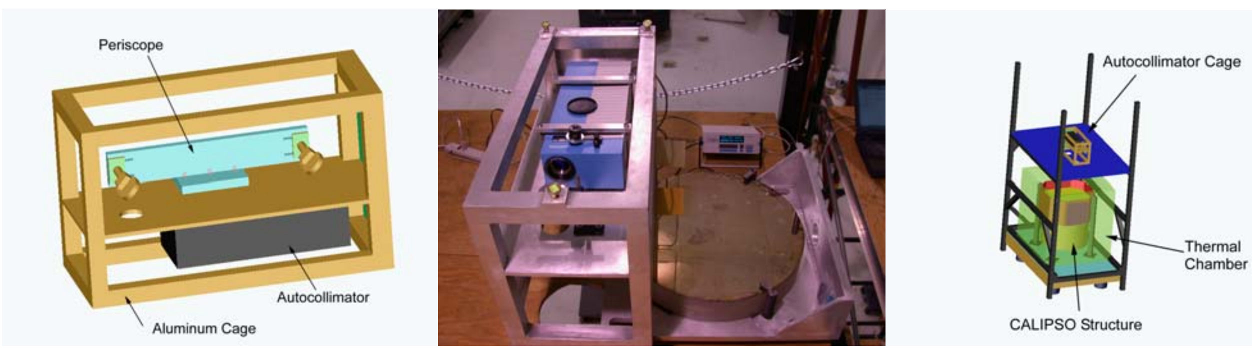

Figure 9: Periscope/Autocollimator Assembly (left), Instrumentation atop Platform (middle), Test Configuration with Tower, Chamber, CALIPSO structure, and Autocollimator Cage Assembly (right)

The boresights of the laser and telescope are separated by approximately 0.5 m. To combine these two parallel boresights into a single instrument configuration, a beam splitting periscope was used. The periscope divided the signal from the autocollimator into two parallel beams that were directed towards the mirrors on the reference fixtures. The beamsplitting element in the periscope was a mirror that covered half of the 50 mm autocollimator beam. Instability in the periscope would compromise the accuracy of the data. A gradient of as little as 0.050 C across a borosilicate periscope would change the reading by 8 μrad. In order to provide a more stable periscope, the metering structure was manufactured from ULE^{TM}. The periscope was mounted in a frame with the autocollimator (see Figure 9). Even with a thermal stable periscope, the autocollimator/periscope assembly had to be calibrated prior to each measurement. A 0.5 m optical flat was used to calibrate the measurement system before each data set was collected.

5. RESULTS FROM THERMAL TEST

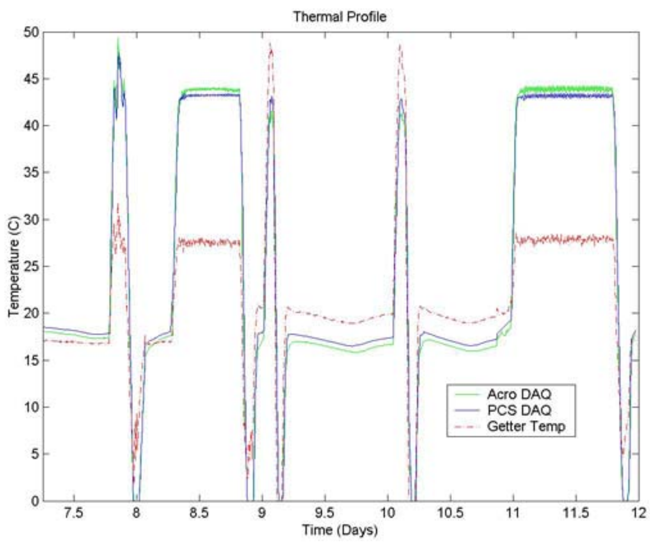

Figure 10: History of Temperature During Thermal Test

The test conditions demonstrated an extremely stable thermal environment. Figure 10 shows the history of the readings of the thermocouples during the test. The temperature range of the thermocouples on the structure was ±2.5 C. A getter was implemented to collect condensables as the structure cooled. This reading is shown in Figure 10 as a dashed line.

The optical bench stability data was analyzed to produce a three dimensional displacement vector for each measurement point. The results are summarized in Tables 1 and 2.

Table 1: Deformation (μm) at 0 C (0 C – RT)

Instrument	dx	dy	dz	dρ
Field Stop	-6.0	9.1	16.5	19.8
PMT	6.2	2.2	-14.3	15.8
APD	1.3	27.0	0.9	27.1
Collimator	-2.7	9.4	-12.2	15.6
Dichroic	2.4	11.5	4.6	12.6
Optics Cube	0.3	-13.0	-23.0	26.5

Table 2: Deformation (μm) at 50 C (50 C – RT)

Instrument	dx	dy	dz	dρ
Field Stop	2.5	-11.9	-25.7	28.5
PMT	-3.7	-31.4	25.4	40.6
APD	-19.0	-6.6	-29.6	35.8
Collimator	7.3	-6.2	37.7	38.8
Dichroic	1.0	-13.9	30.7	33.7
Optics Cube	-4.4	-19.7	52.1	55.8

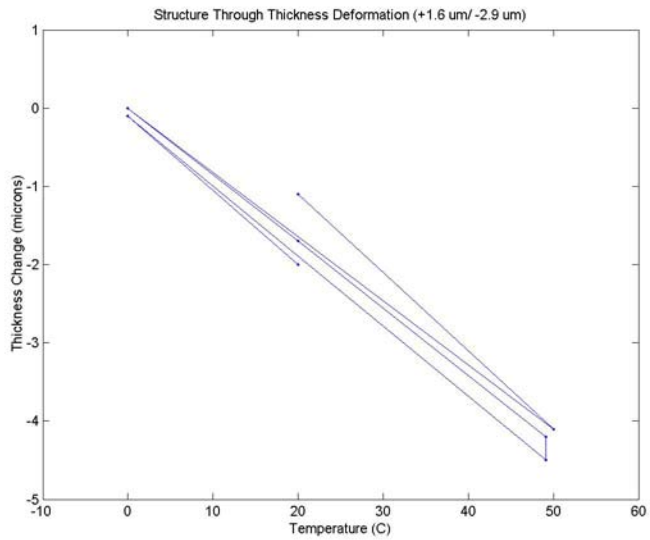

Figure 11: Evolution of Optical Bench Thickness as a Function of Temperature

The optical bench thickness was measured as the average reading of four returns from the laser optical comparator. The progression of thickness as a function of temperature is shown in Figure 11. The structure has a negative coefficient of thermal expansion. Therefore, the optical bench thickness expanded by 1.6 μm when cooled to 0 C and contracted by 2.9 μm when heated to 50 C. There is a small (less than 1 μm) hysteresis evident in the data.

Boresight measurements were collected at four conditions during the thermal cycle: initial room temperature, 0 C, 50 C, and final room temperature. Using the initial room temperature and two extreme temperatures, the stability of the structure was evaluated (see Table 3). Using the initial and final room temperature measurements, the repeatability of the test was calculated. The Θ_x angle refers to a change in the angle perpendicular to the plane that contains the laser and telescope boresights. The Θ_y angle refers to a change in the angle in the plane of the laser and telescope boresights.

Table 3: Boresight Stability Over Temperature

Condition	Θ_x	Θ_y	Magnitude
0 C – RT	3.8 μrad	29.9 μrad	30.1 μrad
50 C – RT	8.2 μrad	-34.8 μrad	35.7 μrad
$RT_2 – RT_1$	3.4 μrad	-4.8 μrad	5.9 μrad

In addition to the excellent repeatability of the room temperature data, the data showed a very small standard deviation for each temperature. The standard deviation did vary with temperature (σ_0 = 2.2 μrad; σ_{50} = 6.5 μrad; σ_{RT} = 1.3 μrad).

6. SUMMARY

A robust set of measurements has shown that the thermal stability performance CFRC structure for the CALIPSO LIDAR compares favorably with the specifications. A series of novel configurations combined with careful calibration and kinematic references contributed to relatively small errors in measurement. The use of reclaimed ULE^{TM} for reference fixtures and use of an ambient pressure test chamber contributed to cost and schedule savings.

7. ACKNOWLEDGEMENTS

The authors wish to thank Stan Backovsky and Mark Mimovich of COI for review of the test procedure and methods. The authors are also grateful for the support of the University of Arizona, specifically Professor Jim Burge and Marty Valente. Prof. Burge provided insightful discussions in the configuration of the test. Marty Valente provided the Elcomat HR autocollimator and 0.5 m flat used for boresight testing. We also thank Pat Bass of Leica Geo-Systems for supporting the characterization of the Leica LTD 500 laser tracker and the loan of special equipment for testing. We also appreciate Tom Lowell's (Vermont Photonics) consultation in the use of the Elcomat HR autocollimator. The authors thank Mitch Brown, Diana Light, Chris Petit, and Carl Weimer of Ball Aerospace for fruitful discussions regarding the specifications, test configuration, and relationship between the test data and performance of the LIDAR. Special thanks to Tony Sorcinelli and Greg McNab at COI for supporting all aspects of the test. This work was performed under contract to Ball Aerospace in support of the CALIPSO LIDAR mission for the NASA Langley Research Center.